Geoid generation and subsurface structure delineation under the Bay of Bengal, India using satellite altimeter data

S. Rajesh and T. J. Majumdar*,†

Physical Research Laboratory, Navrangpura, Ahmedabad 380 009, India
*Marine and Water Resources Group, Remote Sensing Applications Area, Space Applications Centre (ISRO), Ahmedabad 380 015, India

In the present study, Geosat Exact Repeat Mission (ERM) and ERS-1 altimeter data over the Bay of Bengal have been processed for deriving marine geoid and gravity. Processing of altimeter data involves corrections for various atmospheric and oceanographic effects, stacking and averaging of repeat passes, cross-over correction, removal of deeper structures and bathymetric effects, spectral analysis and conversion of geoid into free-air gravity anomaly. The final processed results are available in the form of residual/prospecting geoid and gravity anomaly maps. The highs and lows observed in those maps have been interpreted in terms of a number of prominent mega structures, e.g. gravity linears, 85°E and 90°E ridges, the Andaman trench complex, etc. Satellite-derived gravity contour patterns match well with the available ship-borne results. Also, continental margin as well as 85°E and 90°E ridges could be demarcated well along latitudinal profiles. The isostatic compensation of major crustal features in this region has been discussed in the light of multiple wavelength marine geoid and free-air gravity. Results from the earlier studies using seismological data analysis and modelling also confirm high stress near the Ninetyeast Ridge. In addition, subsurface modelling over 85°E ridge shows that the crustal root has become shallower as one moves from north to south (14°N to 10°N). Progressive shifting of Continent Ocean crustal Boundary (COB) along the eastern passive continental margin has been observed both in satellite-derived and ship-borne gravity data.

SATELLITE altimetry is an efficient reconnaissance tool for offshore hydrocarbon exploration and is also widely used for the regional scale oceanic lithospheric studies. The method uses mass of water as a natural gravimeter, which bulges over mass concentrations such as shallow high density basement features and is depressed over thick low density sediments. Careful efforts must be made to reduce the inherent errors in the measurement of sea surface height. The inferred subsurface geological structures from the sea surface height are analogous to gravity anomaly maps generated through ship-borne survey. A joint collaborative study had recently been completed between SAC (ISRO) and KDMIPE (ONGC) to develop a methodology to use altimeter data as an aid to offshore hydrocarbon exploration and to study the tectonics and related offshore oceanic processes in the Arabian sea and the Bay of Bengal.

Offshore sedimentary basins surrounding India have not been sufficiently explored despite the fact that they contain large-scale hydrocarbon/mineral resources[1]. A satellite altimeter measures the height of the satellite above the instantaneous sea surface with a good precision (~ 5 cm). Precise satellite orbit computations are used to derive the height of the sea surface with respect to a reference ellipsoid, called sea surface height (SSH)[2]. Sea surface height (SSH) measured by Geosat is corrected for various atmospheric and oceanographic effects on the basis of parameters provided in the Geosat/ERS-1 Geophysical Data Record (GDR)[3]. The corrected SSH obtained using Geosat/ERS-1 Exact Repeat Mission (ERM) data for a period of one year is averaged to minimize the effects of dynamic sea surface topography which is mainly due to currents, eddies, etc. This averaged SSH is a good approximation to the classical geoid, which contains information regarding mass distribution in the earth. The anomalies (highs and lows) in geoid surface are directly interpreted in terms of subsurface geological features, e.g. transform faults, fracture zones, basement highs and lows, etc. The geoid anomalies are converted into free-air gravity anomalies, which are particularly useful in deep sea, where traditional ship-borne geophysical data is either unavailable or scanty. In the eastern offshore, India, regional crustal features, e.g. the 85°E ridge, the Central Basin, the Ninetyeast Ridge, the Sunda Arc, the Andaman trench, etc. have been well-defined from ship-borne geophysical survey[4,5]. Hence, mapping those features using satellite-derived geoid/gravity anomalies may be useful for establishing the Satellite Gravity Method. However, though satellite altimeter is a very promising tool, its use requires a number of error-reduction procedures[3,6].

†For correspondence. (e-mail: tjmajumdar@rediffmail.com)

Haxby *et al.*[7] have generated digital images from the combined oceanic and continental data sets and have specified their usages in tectonic studies. Sandwell and McAdoo[8] have applied gradient methods for the analysis of gravity and geoid information. Rapp[9,10] has developed a method for the prediction of gravity anomaly using spherical harmonic coefficients up to degree and order 30 and above. Craig and Sandwell[11] have identified a number of seamounts in the transition zone off Indian coast. McAdoo[12] has generated gravity field of the Southern Ocean from Geosat Exact Repeat Mission (ERM) data. Lundgren and Nordin[13] and Majumdar *et al.*[14] have developed a brief methodology for offshore structure delineation using altimeter data. Long wavelength geoid/gravity has so far not been generated over the Bay of Bengal and hence this work is unique particularly over this region. Also, the earlier workers[5,7,15,16] have used satellite altimeter data to generate the generalized free-air gravity. In this case, Geosat as well as ERS-1 168 day repeat ERM data have been utilized to generate geoid/free-air gravity over the Bay of Bengal and spectral analysis technique has been suitably applied to extract the information regarding different wavelengths of interest.

Data source and area of study

Data over the eastern offshore of India (latitudes: 6°–22°N and longitudes: 77°–95°E) are available from Geosat/ERS-1 ERM. Size of the footprint along the satellite tracks is 6.7 km; however, the cross-track data gap is approximately 150/80 km at the equator for Geosat/ERS-1. Geophysical Data Record (GDR) details are given elsewhere[6,17]. The ship-borne gravity data along with other geophysical/geological information have been used in the study. Bathymetry data used have been obtained from Naval Hydrographic Charts (Survey of India, Dehradun) whereas other ship-borne geophysical data, e.g. gravity, sediment thickness, etc. were collected by ONGC (Dehradun). Geosat data collected over a period of one year have been used in this study. ERS-1, 168/35 day repeat data over the Bay of Bengal have also been processed and used in specific case studies.

Methodology

Geoid is a gravitational equipotential surface approximating to the mean sea surface over the ocean. Sea surface height observations, when averaged, minimizes the effects due to dynamic sea surface topography particularly in regions with seasonally varying currents, such as the Bay of Bengal[18]. The contributions in geoid can be broadly divided into three categories[13,19], viz. bathymetric contribution, lithospheric contribution, and contribution due to deeper earth.

Bathymetry data along the satellite track are used to model the geoid due to bathymetry and then to remove the effects due to bathymetric anomaly. The contributions due to deeper earth are removed using GEM 10B geopotential model expanded up to degree and order 50 (ref. 9). The geoid undulation obtained after removing the contributions due to bathymetry and deeper earth is known as prospecting geoid which corresponds to the mass distribution in the lithosphere. This prospecting geoid is useful in delineating offshore hydrocarbon-bearing structures. Figure 1 shows the flow chart of the data processing scheme used for computation of residual/prospecting geoid and gravity anomaly using altimeter data[19].

Computation of free-air gravity

The fundamental relations useful for conversion of geoid to free-air gravity anomaly can be derived on the basis of the Brun's formula and the equation of the Physical Geodesy[20]. The free-air gravity anomaly can be obtained from the inverse 2D Fourier transform of sum of the slope of the geoid in east component $\eta(\mathbf{K})$ and north component $\xi(\mathbf{K})$ in wave number domain using the relation[15,21],

$$\Delta g(\mathbf{K},0) = \frac{ig_0}{|\mathbf{K}|}[\kappa_x \eta(\mathbf{K}) + \kappa_y \xi(\mathbf{K})], \quad (1)$$

where $\Delta g(\mathbf{K},0) \rightarrow$ Fourier transform of the free-air gravity anomaly in wave number domain κ_x, κ_y, $\mathbf{K} = \sqrt{\kappa_x^2 + \kappa_y^2}$ and $g_0 = 9.8$ m s^{-2} (normal gravity at the point of interest).

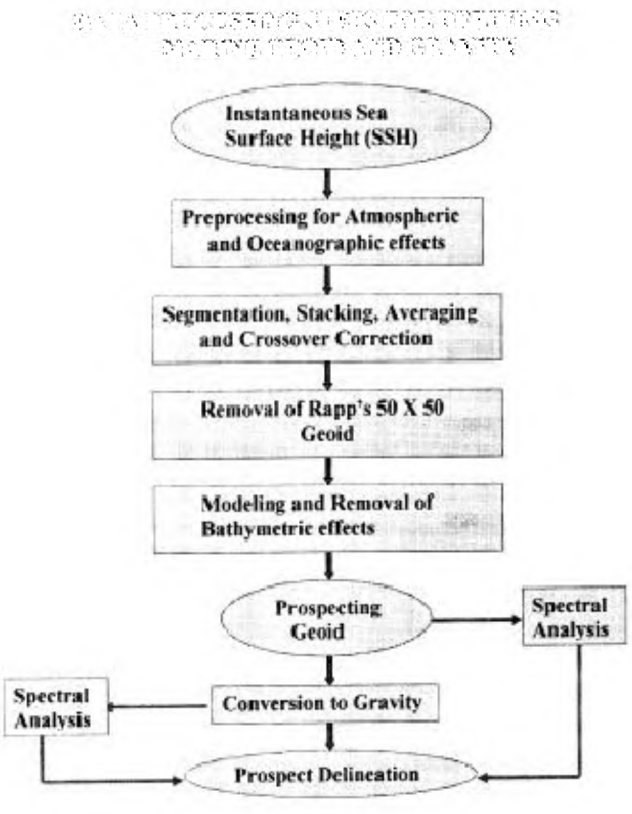

Figure 1. Data processing steps for deriving marine geoid and gravity from satellite altimeter data.

Most topographic loads of wavelengths < 50 km are supported by the strength of the lithosphere and are uncompensated. At wavelengths longer than ~ 500 km, topography is in general locally compensated. Features within the wavelengths (50–500 km) are compensated by the elastic flexure of the upper lithosphere[22]. Different components of the prospecting geoid and free-air gravity anomaly have been obtained using spectral analysis through Fourier transform which can be related with different geological structures[13,19]:

(a) Long wavelength component (100–400 km): It mainly reflects crustal events of regional proportions.
(b) Intermediate wavelength component (50–100 km): It investigates shallower occurrences. These undulations can give information regarding the local isostatic compensation mechanisms and tectonic trend.
(c) Short wavelength component (15–50 km): These undulations are more closely related to basement topography and overlying sedimentary cover.

To compute short, medium and long wavelength components of geoid and gravity, it is assumed that geoid undulation and gravity can be represented by Fourier series[23]. For a one-dimensional finite series, containing N equally spaced observations, only $N/2$ harmonics can be computed with $N/2$th harmonics (Nyquist frequency) corresponding to a wavelength 2Δ, where Δ is the distance between successive observations. First, the coefficients of different harmonics were computed from geoid and gravity values, and then coefficients corresponding to different wavelengths 15–50, 50–100, and 100–400 km were combined and inverse Fourier transformed to calculate short, medium and long wavelength components. Geosat/ERS-1 altimeter data observations along the track are at 6.7 km interval. Therefore, Nyquist frequency will correspond to a wavelength of 13.4 km. The zeroth harmonic will correspond to a wavelength of $N/2$th order and the first harmonic will have wavelength $N/2 \cdot 2\Delta = N \cdot \Delta$. Similarly, other harmonics have been identified to obtain the geoid and gravity values of required wavelengths. For two-dimensional finite series, the above procedure has to be repeated along the latitudinal and longitudinal axes (x, y).

Results and discussion

Classical geoid obtained after the removal of atmospheric and oceanographic effects from sea surface height of Geosat GDR shows smooth contours in the Bay of Bengal (Figure 2). (For security restrictions, lat./ion. coordinates have been omitted in a few maps.) The values range from – 56 m to – 106 m. Higher values are concentrated in the deltaic front of the Ganges and the Brahmaputra and also near the Andaman Islands. The deepest low was found west of Sri Lanka (L_M) whose origin lies in the mantle-core boundary. Continental margin lows (AA′ and BB′ in Figure 2) can be picked up from this map. Linear

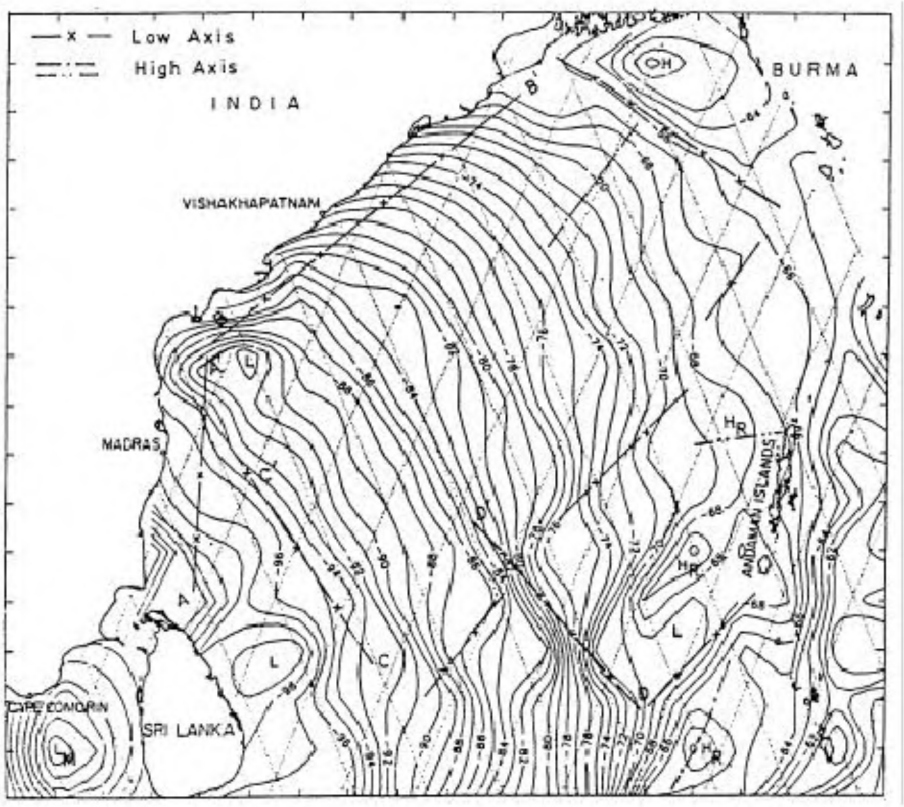

Figure 2. Classical geoid contours (from Geosat) over the Bay of Bengal.

high trends (H_R in Figure 2) near the west of the Andaman Islands were observed. The lateral variation in the mantle density, due to the subducting lithospheric slab near the Andaman Islands, could cause the regional increase in the EW geoid gradient. The geoid signals caused by the lithospheric undulation of Ninetyeast Ridge seems to have overlapped with the broad EW gradient anomaly. A few NW–SE trending linears (CC′ and DD′) have been picked up which are related with deep-seated faults.

Residual geoid anomaly patterns as obtained from ERS-1 altimeter data after correction due to deeper earth mass anomalies along a few profiles are shown in Figure 3. It shows a general downward trend of the basement as one proceeds from 10°N to 14°N latitudes. This downward trend in the basement can possibly attribute to the progressive increase in Bengal fan sediment load at the northern latitudes. Interpretation of bathymetric map obtained from Naval Hydrographic Charts[24], after interpolation illustrates two contrasting bathymetric trends: (i) an observed N–S high trend, which demarcates the Ninetyeast Ridge at the southern latitudes and (ii) the Andaman arc trench low observed east of Ninetyeast Ridge. These two features were seen besides the other morphological features near the eastern Indian continental margin.

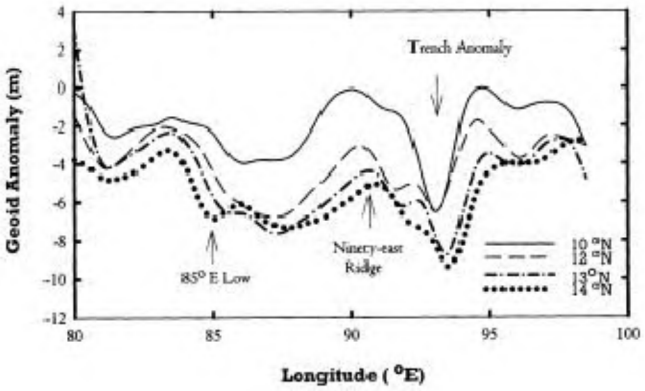

Figure 3. Residual geoid anomalies (from ERS-1) along different profiles in the Bay of Bengal.

Prospecting geoid contour map

The prospecting geoid anomaly map over the study area, after the removal of bathymetry and deeper earth effects, is shown in Figure 4. Contours as such do not follow any particular trend. Various isolated geoid lows (L) and highs (H) were observed, in the general background of low geoid value towards the northern latitudes. Low axis (marked in Figure 4) of most of the NE–SW trending linear features of the basin may represent the distributary channels for sedimentary deposition. Lows near the Bengal fan mouth and Andaman Islands represent greater sedimentary thicknesses in the Bengal fore deep and the Andaman trenches. The clustering of isolated lows at the central portion of the basin suggests flexure of the basement due to sediment

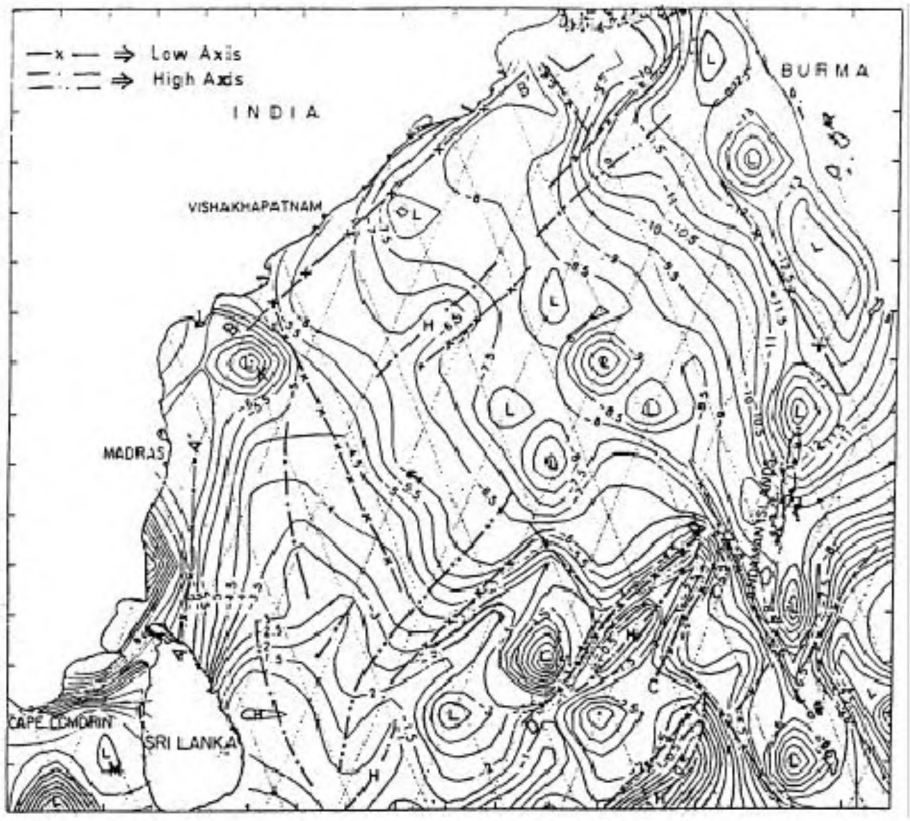

Figure 4. Prospecting geoid contour map over the Bay of Bengal (from Geosat).

load. The linear geoid high trend at roughly southeast of the central basin laws is due to the Ninetyeast Ridge. The ridge seems to have been disseminated and bounded by NE–SW trending faults at its flanks (CC′ and DD′) which is also supported by bathymetric features. Seismic profiles by Curray *et al.*[25] have shown that the Ninetyeast Ridge is a basement high feature.

Analysis along the passive eastern continental margin has shown two major linear geoid lows, namely, AA′ and BB′. AA′ has a N–S trend from the north of Sri Lanka to Krishna basin (North of Madras) in the southeastern part of India and BB′ has a NE–SW trend from Godavari basin to the mouth of the Bengal fan delta[26]. A prominent low (L_K in Figure 4) has been observed off Krishna–Godavari offshore between the mapped continental margin lows (AA′ and BB′), which indicates a major depression in the basement with large fan sediments.

Long wavelength (100–400 km) prospecting geoid undulation

The longer wavelength prospecting geoid information in the spatial wavelength band 100–400 km is shown in Figure 5. The low anomaly closures, 'L', are those lithospheric features which are undergoing regional isostatic compensation. These regions have nonzero geoid anomalies and are a measure of density distribution with depth and hence it illustrates the mechanism of compensation of the lithosphere. Here the values range from 15 m to – 15 m. This suggests a northward down buckling of the oceanic crust due to the large thickness of sediment in this region. Lineaments based on contour gradients are marked, and prominent trends are nearly E–W (E_1E_2, E_3E_4), NE–SW (N_1N_2, N_3N_4), NW–SE (S_1S_2), and NNW–SSE (W_1W_2). The prominent lithospheric feature at the Ninetyeast Ridge is seen as a roughly NS high linear feature bounded by the trends E_1E_2, E_3E_4, S_1S_2 and W_1W_2. These linear trends surrounding the ridge may partly facilitate the vertical movement of the ridge in order to achieve the isostatic stability.

Interpretation of gravity anomalies

Over the past two decades, several authors have prepared gravity anomaly maps over the northeastern Indian ocean and the Arabian sea[16,27–31]. The gravity anomaly values along the eastern offshore mainly range from 50 mGal to – 50 mGal, and the general trend of contours are NW–SE except at the boundary zones near 6°N latitude[14]. Figure 6 shows the ship-borne free-air gravity anomaly along three profiles near continental margin, namely, 10°, 13° and 14°N. The gravity anomaly low along these profiles

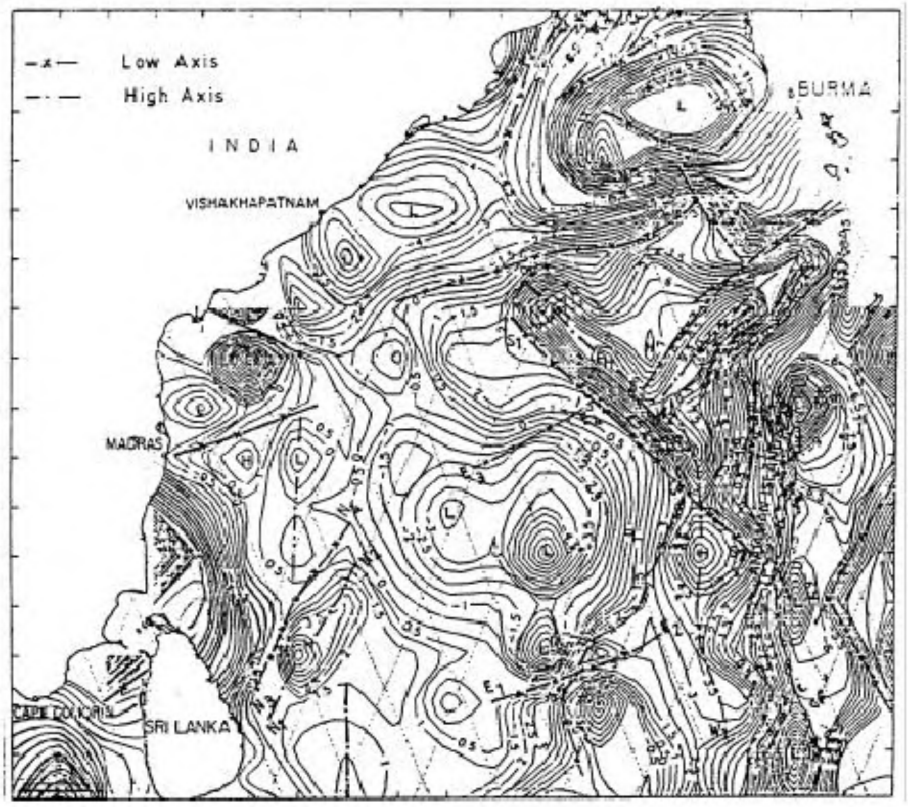

Figure 5. Long wavelength (100–400 km) prospecting geoid contour map over the Bay of Bengal (from Geosat).

shifts towards east as one proceeds from 14° to 10°N latitude. Similar trend has been observed along the eastern continental margin as obtained from satellite-derived gravity[14]. This signifies the progressive shift of the Continental Ocean crustal Boundary (COB) towards east. The GEOSAT derived free-air gravity anomaly map, shown in Figure 7, could clearly demarcate this crustal transition zone throughout the eastern continental margin of India (KK′ and MM′). At the central basin, the anomaly contours are broad and low (L), which can be attributed to the basin depression due to greater fan sediment load. The Ninetyeast Ridge, observed as disseminated, has roughly NS trending linear highs marked as H_1H_2, H_3H_4 and H_5H_6. The NE–SW trending gravity linear marked as L_1L_2 seems to cut across the NS trending H_1H_2 section of the ridge. The orientation of gravity linear and the ridge dissemination, especially between H_1H_2 and H_3H_4 sections suggests a complex tectonic scenario, which arises due to the consequence of oblique subduction processes in the Andaman arc trench system. Besides L_1L_2, other linear trends are also observed in NE–SW and NW–SE directions.

Ramana *et al.*[32] have analysed marine magnetic (ship-borne) data in the northern Bay of Bengal. The analysed magnetic map depicts four magnetic anomaly provinces corresponding to (i) 85°E ridge complex, (ii) newly identified approximately NNE–SSW trending basement high/ridge system, (iii) the 90°E ridge, and (iv) the Sunda trough. Prominent trends observed in this region are N–S and NNE–SSW. Mukhopadhyay[33] has also reported high density anomalous mass underneath the Sunda trough (near Andaman Islands). The Bay of Bengal lithosphere is also characterized by an extraordinary level of intraplate seismicity, as explained by occurrences of earthquakes of magnitude 7 near the Ninetyeast Ridge[34]. Later, Stein *et al.*[35] have also studied the ridge seismicity and observed that, earthquake mechanisms along the Ninetyeast Ridge are generally consistent with the left lateral strike-slip motion. Stein and Okal[34] suggested that a relative motion of the oceanic crust exists in the subduction zone of northeastern Indian Ocean region (Indian side) with respect to the subduction zone in the southern Sumatra trench region (Australian side). The relative motion of the oceanic crust from the Indian side encounters greater resistance to subduction due to Himalayan collision, while the Australian side subducts smoothly at the Sumatra trench. Further insight may be derived from tectonic models such as the finite element calculation of the theoretical stress field for the Indian plate[36]. The predicted high stress near the Ninetyeast Ridge is consistent with the earthquake focal mechanism. Similar results have been reported by Rajesh[37], where it has been interpreted through seismic studies, that a shallow graben-likes structure exists along the ridge axis. From ship-borne gravity it has been observed that the ridge system is shallower towards south and wider at north with an N–NNE trending. Origin of the Ninetyeast Ridge system is associated with the movement of Indian plate over the Kergulean hotspot[38].

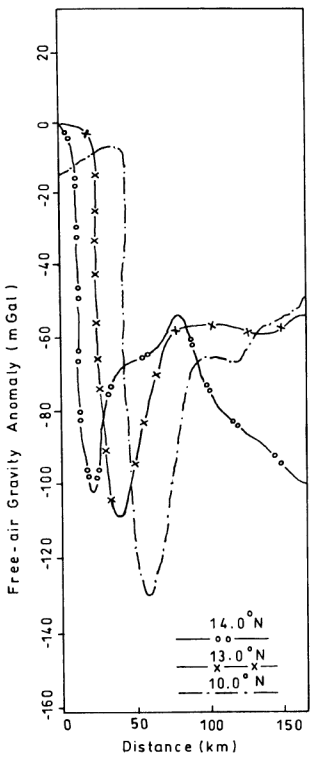

Figure 6. Gravity anomaly (ship-borne) over continental ocean crustal boundary (COB).

Detailed study has been made for the generation of Moho depth near 85°E ridge along three profiles using ship-borne data with the Werner's deconvolution model[39]. E–W profiles have been generated along 10°, 13° and 14°N longitudinal lines. Comparison of satellite-derived gravity with ship-borne gravity data along 10°N profile shows similar trends, especially near the trench and the ridge anomalies shown in Figure 8. Figure 9 shows the results (subsurface lithospheric anomalies as well as basement and Moho depth) as obtained using 2D forward model, with seismic constraints in the thickness of sedimentary layer, along 10°N latitude. Comparison of changes of Moho depth is obtained by assuming the Airy local isostatic compensation of 85°E ridge from 10°N to 14°N as shown in Figure 10. This concludes that the crustal root of 85°E ridge system becomes shallower as it extends from north to south along the axis of 85°E ridge.

Long wavelength (100–400 km) satellite-derived gravity

Figure 11 shows the long wavelength (100–400 km) component of the ERS-1-derived gravity. These long wavelength gravity anomalies are produced by features affected by the density contrasts in the lower crust and the upper-

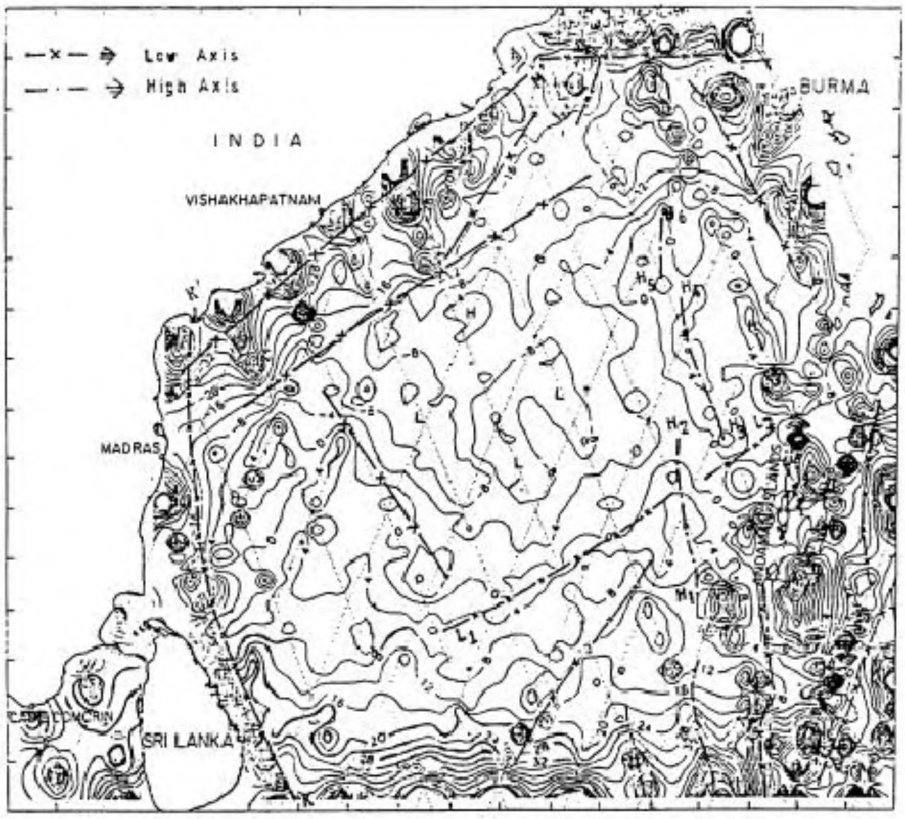

Figure 7. Satellite-derived free-air gravity anomaly map over the Bay of Bengal (from Geosat).

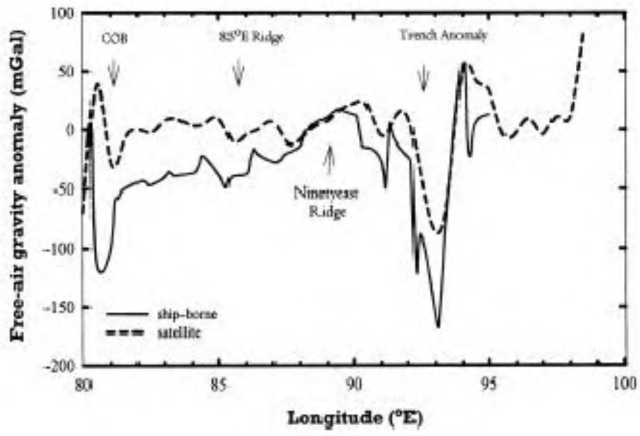

Figure 8. Comparison of ship-borne gravity with satellite-derived (ERS-1) free-air gravity along 10°N profile in the eastern offshore.

most mantle. The general contour trends of long wavelength gravity anomaly (100–400 km) are NE–SW along the Ninetyeast Ridge and its eastern flanks, while most of the crustal local features have NW–SE trend at its western flank. The contour values generally range from 120 mGal to – 80 mGal, with areas of positive and negative anomalies well demarcated. The Ninetyeast Ridge is observed as NE–SW trending broad feature (RR′) with isolated gravity high zones. In this spatial wavelength band, at the central basin and near the Ninetyeast Ridge, the free-air anomaly of most of the features range from – 10 to 10 mGal and those lithospheric features are in a state of near-isostatic compensation. Krishna–Godavari basin low (L) has also been demarcated. Several linear features were picked up from the contour map and the contour gradients which may be related to the major faults/deep crustal heterogeneities[14]. Broad gravity low trends along the margin match with the ship-borne gravity patterns as shown in Figure 6, which represents the transition zone of continental ocean crustal boundary.

Conclusions

From the above study, the following conclusions could be made:

(a) Satellite altimeter data have been used to successfully derive the marine geoid and gravity and their various wavelength components for mapping the megastructures in the Bay of Bengal region and validated with the available ship-borne data[40].

(b) Geoid undulation and free-air gravity anomaly variation observed in this region indicate the presence of a number of highs and lows in the basement rock along with major aseismic ridges as lithospheric loads.

(c) The Ninetyeast Ridge is observed as a basement high in gravity as well as in the prospecting geoid contour maps. The geoid anomaly could effectively reflect the disseminated nature of the ridge crust, even in areas of very high sediment thickness in the northeastern region, where it juxtaposes the Andaman trench.

(d) The observed Andaman trench geoid anomalies are very narrow and less negative amplitude towards southern latitudes. The narrowness in the anomaly can be attributed to greater horizontal ridge push exerted towards east (trench side) as a consequence of oblique subduction, while the reduced negative anomaly is due to relatively less sediment load in this region. The geoid signal low of the Sunda–Andaman trench axis is discontinued by NE–SW trending linear features.

(e) Nearly N–S, NE–SW and NW–SE gravity linears are prominent in the entire Bay of Bengal, and progressive shifting of the continent ocean crustal boundary towards east has been observed along the eastern continental margin of India.

(f) The geoid signal obtained across 10°N to 14°N latitude profiles indicates that the causative (lithosphere) depth is increasing progressively from 10° to 14°N owing to the high sedimentation load from the Bengal Fan.

(g) The free-air gravity anomaly over 85°E ridge is low, as expected with low amplitude, but showing a profile-wise trend along NW direction. Also, the crustal root of 85°E ridge system becomes shallower along the axis of the ridge as it extends from north to south.

(h) The long wavelength gravity anomalies in the 100–400 km spectral band have been produced by features affected by the density contrasts in the lower crust and

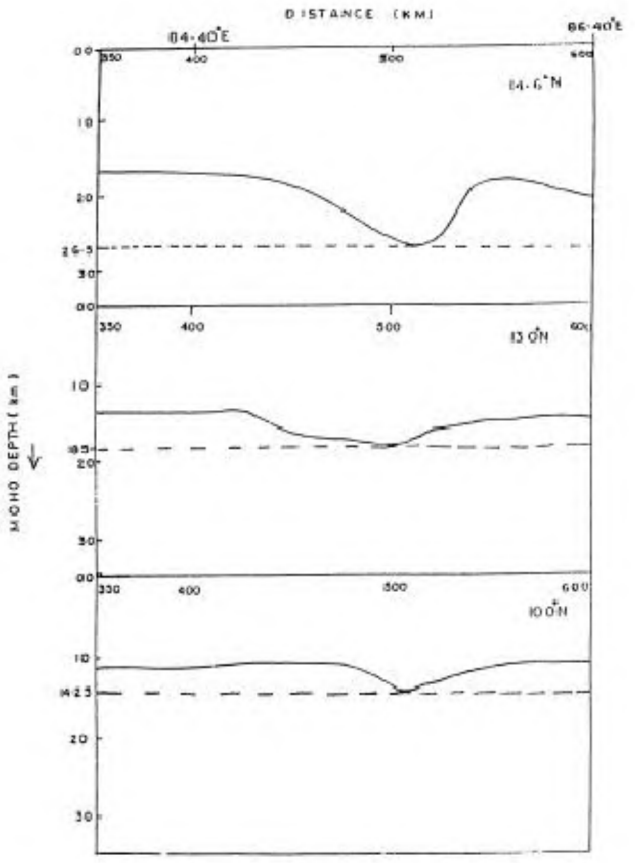

Figure 10. Comparison of Moho depths over 85°E ridge.

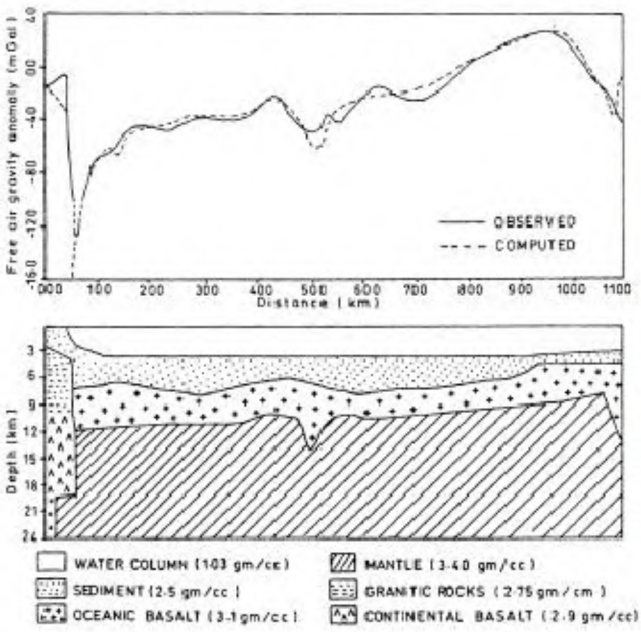

Figure 9. Subsurface lithospheric anomalies as obtained by 2-D Forward Model.

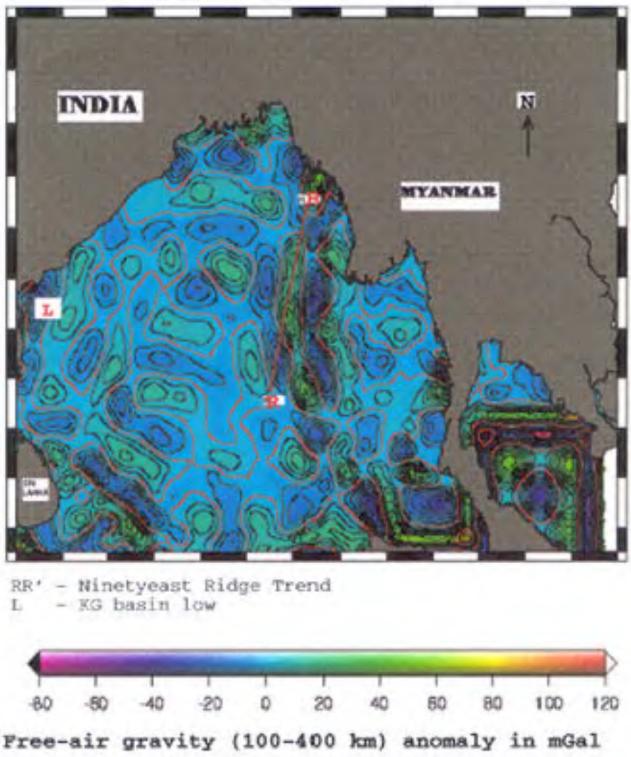

Figure 11. Long wavelength (100–400 km) free-air gravity anomaly contour map over the Bay of Bengal (from ERS-1).

the uppermost mantle. The general contour trends are NE–SW along the Ninetyeast Ridge and its eastern flanks, while most of the other features in the region are in near state of crustal compensation.

1. Biswas, S. K., *AAPG Bull.*, 1982, **66**, 1497–1513.
2. Fu, L. L., Chelton, D. B. and Zlotnicki, V., *Oceanography*, 1988, **1**, **2**, 4–11, 58.
3. Wakker, K. F., Zandbergen, R. C. A., Van Geldorp, G. H. M. and Ambrosius, B. A. C., *Int. J. Remote Sensing*, 1988, **9**, 1797–1818.
4. Ramana, M. V. *et al.*, *J. Geophys. Res.*, 1997, **102**, 17995–18012.
5. Subrahmanyam, V., Krishna, K. S., Radhakrishna Murthy, I. V., Sarma, K. V. L. N. S., Desa, M., Ramana, M. V. and Kamesh Raju, K. A., *Earth Planet. Sci. Lett.*, 2001, **192**, 447–456.
6. Cheney, R. E., Douglas, B. C., Agreen, R. W., Miller, L., Porter, D. L. and Doyle, N. S., *Geosat Altimeter Geophysical Data Record User Handbook*, NOAA Technical Memorandum NOS NGS-46, Rockville, USA, 1987, p. 28.
7. Haxby, F., Karner, G. D., La Brecque, J. L. and Weissel, J. K., *EOS Trans. Am. Geophys. Union*, 1983, **64**, 995–1004.
8. Sandwell, D. T. and McAdoo, D. C., *J. Geophys. Res.*, 1988, **93**, 10389–10396.
9. Rapp, R. H., A Fortran program for computation of gravimetric quantities from high degree spherical harmonic expansions, Rep. No. 334, Department of Geodetic Science and Surveying, The Ohio State University, Columbus, Ohio, Sept. 1982, p. 23.
10. Rapp, R. H., *J. Geophys. Res.*, 1983, **88**, 1552–1562.
11. Craig, C. H. and Sandwell, D. T., *J. Geophys. Res.*, 1988, **93**, 10408–10420.
12. McAdoo, D. C., *J. Geophys. Res.*, 1990, **95**, 3041–3047.
13. Lundgren, B. and Nordin, P., *Satellite Altimetry – A New Prospecting Tool*, 6th Thematic Conference, Colorado, Environmental Institute of Michigan, USA, 1988, pp. 565–575.
14. Majumdar, T. J., Mohanty, K. K. and Srivastava, A. K., *Int. J. Remote Sensing*, 1998, **9**, 1953–1968.
15. Sandwell, D. T. and Smith, W. H. F., *J. Geophys. Res.*, 1997, **102**, 10039–10054.
16. Subrahmanyam, C., Thakur, N. K., Gangadhara Rao, T., Khanna, R., Ramana, M. V. and Subrahmanyam, V., *Earth Planet. Sci. Lett.*, 1999, **171**, 237–251.
17. *ERS-1 Altimeter Data User's Handbook*, ESA Publication Division, France, 1993, p. 140.
18. Stewart, R. H., *Methods of Satellite Oceanography*, University of California Press, California, USA, 1985, pp. 360.
19. Majumdar, T. J., Mohanty, K. K., Sahai, B., Srivastava, A. K., Mitra, D. S. and Agarwal, R. P., Procedure manual for determining gravity from spaceborne altimetric measurements and its use in oil exploration. Tech. Rep. No. SAC/RSA/RSAG/MWRD/TR/01/94, SAC, Ahmedabad, December 1994, p. 72.
20. Moritz, H., *Advanced Physical Geodesy*, Abacus Press, Tun Bridge, Wells Kent, England, 1980, p. 500.
21. Chapman, M. E., *J. Geophys. Res.*, 1979, **84**, 3793–3801.
22. Fu, L. L. and Cazenave, A. (eds) *Satellite Altimetry and Earth Sciences – A Handbook of Techniques and Applications*, Academic Press, San Diego, USA, 2001, p. 463.
23. Farelly, B., *Bull. Geodesique*, 1991, **65**, 92–101.
24. Naval Hydrographic Charts, Naval (Currently, National) Hydrographic Office, Survey of India, Dehradun, 1972.
25. Curray, J. R., Emmel, F. J., Moore, D. G. and Raitt, R. W., in *The Ocean Basins and Margins* (eds Nairn, A. E. M. and Stehli, F. G.), Plenum Press, New York, 1982, vol. 6.
26. Srivastava, A. K., Dotiwala, F., Mitra, D. S., Majumdar, T. J. and Mohanty, K. K., ISRO-ONGC Joint Report, 1994, p. 60.
27. Kahle, H. G. and Talwani, M., *Geophysics*, 1973, **39**, 167–187.
28. Liu, C. S., Sandwell, D. T. and Curray, J. R., *J. Geophys. Res.*, 1982, **87**, 7673–7686.
29. Mukhopadhayay, M. and Krishna, M. R., *Tectonophysics*, 1991, **86**, 365–386.
30. Subramanium, C. and Singh, R. N., *Indian J. Petrol. Geol.*, 1992, **1**, 161–180.
31. Udintsev, G. B., Fisher, R. L., Kanev, V. F., Laughton, A. S., Simpson, E. S. W. and Zhiv, D. I., *Geological and Geophysical Atlas of the Indian Ocean*, Academy of Sciences of USSR, Moscow, 1975.
32. Ramana, M. V. *et al.*, Proceedings of the International Symposium on the Oceanography of Indian Ocean (ISOIO), Goa, 14–16 January 1991, Oxford & IBH, New Delhi, pp. 519–525.
33. Mukhopadhayay, M., *Mar. Geophys. Res.*, 1988, **9**,197–210.
34. Stein, S. and Okal, E. A., in *Space Geodesy and Geodynamics* (eds Anderson, A. J. and Cazenave, A.), Academic Press, London, 1986.
35. Stein, C. A., Cloetingh, S. and Wortel, R., *Geophys. Res. Lett.*, 1989, **16**, 823–826.
36. Cloetingh, S. and Wortel, W., *Geophys. Res. Lett.*, 1985, **12**, 77–80.
37. Rajesh, S., M.Sc. (Tech.) Dissertation, Department of Marine Geology and Geophysics, Cochin University of Science & Technology, Cochin, June 1998, p. 60.
38. Mahony, J. J., Macdougall, J. D., Lugmair, G. W. and Gopalan, K., *Nature*, 1983, **303**, 385–389.
39. Telford, W. M., Geldart, L. P. and Sheriff, R. E., *Applied Geophysics*, Cambridge University Press, Cambridge, 2nd edn, 1991.
40. Majumdar, T. J., Mohanty, K. K., Mishra, D. C. and Arora, K., *Curr. Sci.*, 2001, **80**, 542–554.

ACKNOWLEDGEMENTS. We thank two anonymous referees for their valuable comments for the improvement of this paper. We also thank Dr K. N. Shankara, Director, SAC and Prof. G. S. Agarwal, Director, PRL for their keen interest in this study. We are grateful to Dr S. R. Nayak, Group Director, MWRG/RESA and Prof. R. Ramesh, PRL for their help and encouragements during the course of this study. Ship-borne data were obtained courtesy to Dr V. Ramaswamy, KDMIPE, ONGC, Dehradun.

Received 29 April 2002; revised accepted 17 March 2003